Solid State Communications 174 (2013) 50–54

Contents lists available at ScienceDirect

Solid State Communications

journal homepage: www.elsevier.com/locate/ssc

Analogy of plasmon induced transparency in detuned U-resonators coupling to MDM plasmonic waveguide

Shiping Zhan [a], Deming Kong [a,*], Guangtao Cao [b], Zhihui He [a], Yun Wang [a], Guojun Xu [a], Hongjian Li [a,b,*]

[a] College of Physics and Electronics, Central South University, Changsha 410083, China
[b] College of Materials Science and Engineering, Central South University, Changsha 410083, China

ARTICLE INFO

Article history:
Received 22 May 2013
Received in revised form
6 September 2013
Accepted 13 September 2013
by R. Phillips
Available online 20 September 2013

Keywords:
D. PIT-like
E. Coupled-mode theory
C. MDM waveguide
C. Wavelength detuning.

ABSTRACT

We provide an investigation on the analogy of plasmon induced transparency (PIT) in plasmonic waveguide numerically and theoretically. A simplified Coupled-Mode theory model is used to demonstrate the PIT-like effect in a system consisting of two detuned U-resonators (DURs) back coupled to a metal–dielectric–metal (MDM) waveguide. The detuned wavelength δ is introduced by the simplified model qualitatively due to the structural design. The sensitivity of wavelength and the trade-off between *Q*-factor and transmission maxima are considered. Finally, the observed slow light effect in our system guarantees a low group velocity which has potential application in nano-filter and optical buffer.

1. Introduction

Metamaterials possess extended unprecedented abilities to manipulate electromagnetic waves and potential applications which have attracted significant research interest recently [1–4]. Electromagnetically induced transparency (EIT) is a special and counterintuitive phenomenon which occurs in energy level atomic systems due to the quantum destructive interference between the excitation pathways to the atomic upper level consequently, which leads to an elimination of absorption over a narrow spectral region in a broad absorption regime [5,6]. The EIT-associated features of strong dispersion and slow-light propagation within the transparency window [7,8], may guarantee a potential application in optical buffer and optical storage. However, owing to the required specific and strict restrictions, the further realization of original atomic EIT is constrained. Surface plasmon polaritons (SPPs), trapped on the metal–insulator–metal interface, are regarded as one of the most promising technologies for the minimization of on-chip integrated devices owing to their capabilities to overcome the classical diffraction limit and manipulate light in the nanoscale domain [9–11]. Recent studies have shown that the plasmon induced-transparency (PIT) can provide a non-quantum analogy of EIT feature, which has the advantages of room-temperature manipulability and the ability to integrate with nanoplasmonic circuits. A number of classical configurations have been suggested for the realization of PIT-like, including coupled dielectric resonators [12,13], metamaterial-induced transparency [14] phase-coupled plasmon-induced transparency [15], EIT-like effect in split-ring resonators [16,17] and in detuned stub resonators [18]. Because of the inherent property of strong field confinement, plasmonic devices such as MDM waveguide are more promising in fabricating structures with ultracompact sizes. The PIT can be achieved due to the cancelation of opposite contributions from two detuned resonances, which are equally spaced but with opposite signs of detuning from the probe frequency (with the detuning being close to the resonance linewidth), resulting from the Fano-like interference of the decay channels [19]. Two metal stripes with difference in length placed on top of a Si waveguide are used as phase-coupled surface plasmon resonators that would ensure EIT-like transmission [15]. Using detuned resonators that are both coupled to a bus waveguide can also be beneficial for the realization of PIT-like phenomenon [20]. Also, for better understanding of EIT-like feature in MDM structure, some theoretical researches are investigated, such as Coupled-mode theory (CMT) [21] and transmission line theory [22].

In this paper, the plasmon induced-transparency feature is verified by investigating the detuned back coupled U-resonators in MDM plasmonic waveguide. We consider that the degree of detuning obviously affects the quality-factor(QF) and transmission peak of the transparency window. Due to the near-field evanescent wave coupling, the QF and extinction ratio is relatively higher than that in Ref.

* Corresponding authors at: College of Physics and Electronics, Central South University, Changsha 410083, China. Tel.: +86 731 88836457; fax: +86 731 88877805.
E-mail addresses: kong1971@163.com (D. Kong), lihj398@csu.edu.cn (H. Li).

0038-1098/$ - see front matter © 2013 Elsevier Ltd. All rights reserved.
http://dx.doi.org/10.1016/j.ssc.2013.09.013

[23].The U-resonators in MDM resonate in (out) phase result in a low (high) transmission. A modified CMT equation is introduced to get further investigation of the PIT-like spectra. Finally the slow-light effect is studied in our structure with an approximately achieved group index, which leads to the group velocity of incident pulse nearly two orders slower than that in vacuum. This pronounced slow light effect can be beneficial in nano-filters, optical switchs, and slow-light systems and devices, especially optical buffers.

2. Geometry and numerical simulating

Fig. 1 illustrates the geometry of the detuned back coupled U-resonators in MIM plasmonic waveguide structure. The upper U-resonator has arm length L_1, width w and horizontal length L, while the lower U-resonator has arm length L_2 and shares the same width w and horizontal length L. The MDM waveguide is set to be embedded in the middle of the two resonators with a certain vertical gap distance d for both of them.

The background metal is chosen to be gold (Au), of which the frequency dependent dispersive permittivity is approximately defined by the Drude model, as

$$\varepsilon(\omega) = 1 - \frac{\omega_p^2}{\omega^2+\gamma_p^2} + i\frac{\omega_p^2\gamma_p^2}{\omega(\omega^2+\gamma_p^2)} \quad (1)$$

where $\omega_p = 1.37\times10^{16}\ s^{-1}$ is the bulk plasmon frequency, ω stands for the angle frequency of the incident wave, and $\gamma_p = 4.08\times10^{13}\ s^{-1}$ represents the damping rate which characterises the absorption loss. These values are obtained by fitting the experimental results [24]. The dielectric spacer is chosen to be air with permittivity $\varepsilon_d = 1$ for simplicity, which has no influence on the PIT-like feature except for blueshift or redshift and does not lead to any loss of generality in the discussion later.

The characteristic spectral responses of the chosen structures are performed by the two dimensional Finite-Difference Time-Domain (FDTD) method [25]. We simulate the structure with an FDTD lattice of size $L_x \times L_y = 800\ nm \times 800\ nm$, the spatial and temporal steps are set as $\Delta x = \Delta y = 2.5$ nm, and $\Delta t = \Delta x/2c$ ($c$is the velocity of light in vacuum). The perfectly matched layer (PML) absorbing boundary conditions are used for computational space along both x and y directions. A Gaussian single pulse of light with wide frequency profile and only normally incident p-polarized plane-waves are considered here, implying that the magnetic field is parallel to the slits (along the z direction). Finally, the calculated transmission spectra are normalized by the calculation without a metallic structure.

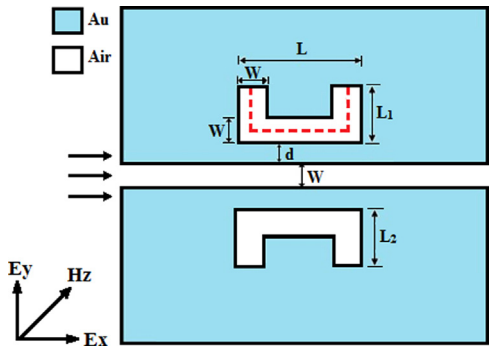

Fig. 1. (Color online) The geometry of the detuned back coupled U-resonators in MDM plasmonic waveguide structure.

3. Result and discussion

3.1. Side-coupled U-resonator

Fig. 2(a) shows the transmission spectra of a single U-resonator coupling to the bus MDM waveguide, where the parameters are given as follows: $L = 280$ nm, $w = 50$ nm, $d = 20$ nm which are kept constant throughout this research while $L_1 = 115$ nm and $L_2 = 135$ nm. Transmission dips centered at 1242 nm and 1314 nm can be observed from the image. The mentioned U-shaped cavity can be approximatively regarded as a Fabry–Perot resonator with high reflectivity at the end due to the small skin depth [26]. In our structure, the optical path difference per roundtrip is $2L_{eff}n_{eff}$, where L_{eff} is the effective length of the U-resonator, which is marked as a red dash line in Fig. 1, and n_{eff} is the effective index of the MDM waveguide. So the phase delay per round-trip for the nanocavity can be given as [27]: $\Delta\Phi = 2\pi(2L_{eff}n_{eff})/\lambda + 2\varphi$, where φ is phase shift of a beam reflected on air–gold interfaces. Thereby the resonant conditions can be expressed as: $\Delta\Phi = m2\pi$, integer m represents the mode order of the cavity. Then the resonant wavelength λ_m can be derived as follows: $\lambda m = 2L_{eff}n_{eff}/(m-\varphi/\pi)$.

For the resonant wavelength of 1242 nm in Fig. 2(a), one can calculate the effective length of the U-resonator to be $(L_{eff})_{cal} = 418$ nm when m equals 1, which is very close to the designed $(L_{eff})_{des} = 410$ nm. Similarly the resonant wavelength of 1314 nm is $(L_{eff})_{cal} = 461$ nm while the designed $(L_{eff})_{des} = 450$ nm. The small difference between the simulated and calculated values can be attributed to the approximation of n_{eff} and the phase shift caused by the near-field evanescent wave coupling. Even then, the equations displayed above are still beneficial for the rough design of plasmonic device.

3.2. PIT-like feature in back coupled DURs

When these two U-resonators with arm length $L_1 = 115$ nm and $L_2 = 135$ nm, $L_1 + L_2 = 250$ nm and other parameters are kept constant as above description, are combined as the inset of Fig. 2(b) shows, a transmission peak at $\lambda_3 = 1284$ nm with a quality-factor of almost 25 and two resonant dips at $\lambda_1 = 1242$ nm and $\lambda_2 = 1314$ nm are all obs-
erved, which indicates that a pronounced PIT feature is acquired in this structure. The transmission peak does not reach 100% as the existent metal loss causes a finite lifetime in the resonator.

It is clear from the field analysis that these two resonant dips λ_1 and λ_2 are corresponding to the upper and lower resonators, respectively. While the PIT-like peak λ_3 is achieved due to the cancelation of opposite contributions from two detuned resonances related to the upper and lower U-resonators.

In order to elucidate the electromagnetic response of the detuned back side-coupled U-resonators, the Coupled-Mode Theory (CMT) is utilized to investigate this PIT-like phenomenon theoretically. Here, we neglect the coupling between the two resonators due to the structural design which means an indirect coupling here. The complex transmission t_n and reflection coefficient r_n for single U-shaped resonator can be obtained from the previous work as follows [12]:

$$t_n = (i(\omega_n-\omega)+\gamma_{on})/(i(\omega_n-\omega)+\gamma_n) \quad \text{and}$$
$$r_n = -\gamma_{en}/(i(\omega_n-\omega)+\gamma_n), \quad (n=1,2) \quad (2)$$

where ω_n is the resonant frequency of the resonator, $\gamma_{on} = \pi c/(\lambda_n Q_{on})$ and $\gamma_{en} = \pi c/(\lambda_n Q_{en})$ are the decay rates corresponding to the internal loss and the coupling loss to the waveguide of the nth resonator, respectively. Q_o is the intrinsic quality factor which can be described as [28] $Q_o = \mathrm{Re}(n_{eff})/2\mathrm{Im}(n_{eff})$, where the expression of refractive index n_{eff} can be found in [29].Under the condition of $1/Q_o \ll 1/Q_e$,

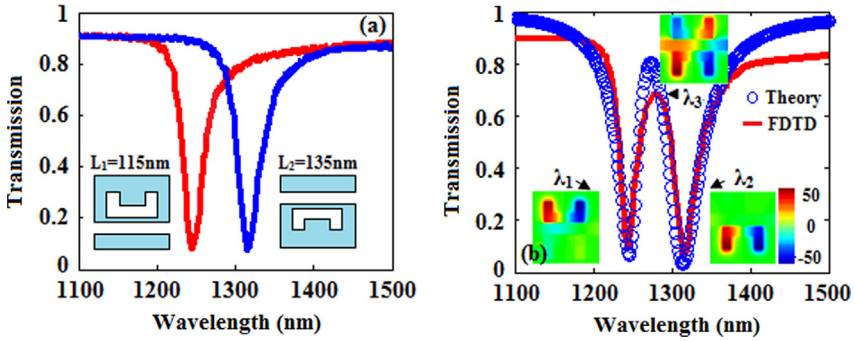

Fig. 2. (Color online) (a) The transmission spectra for single side-coupled U-resonator, (b)The simulation result and Coupled-mode theory result for combined side-coupled DURs with $L_1=115$ nm and $L_2=135$ nm while $L=280$ nm, $w=50$ nm, $d=20$ nm.The insets are magnetic field distributions for $\lambda_1=1242$ nm, $\lambda_2=1314$ nm, $\lambda_3=1284$ nm, respectively, and the color scales for the field distribution in all insets are the same.

there is a relationship among Q_t,Q_o and Q_e, as$1/Q_t=1/Q_o+1/Q_e$ [12]. Where Q_t is the total quality factor and can be evaluated from the formula that $Q_t=\lambda/\Delta\lambda$, wavelength λ and $\Delta\lambda$ are corresponding to the resonance wavelength and full width of half maximum (FWHM).

The system proposed in this paper can be regard as a Fabry–Perot resonator with two frequency-dependent mirrors [15] with resonator–resonator phase shift $\phi_{r-r}=0$ due to the structural design. Then the total transmission efficiency can be derived as

$$T=\left|\frac{t_1t_2}{1-r_1r_2}\right|^2 \tag{3}$$

The theoretical transmission spectra is shown in Fig. 2(b) in orange circle, which approximately agrees with the FDTD result except for some difference in the transmission values which may result from the rough approximation of Q_e and Q_t as well as the near-field evanescent wave coupling. The extinction ratio for the simulated spectra is approximated to be 0.89 while ~1 for the theoretical one. However, both the theoretical and simulated results provide a similar profile, and this modified equation can be significant in understanding the PIT-like spectra in a certain extent with a more concise form.

For better understanding of the PIT-like feature and the internal physical mechanism, the distribution of magnetic field for the back coupled DURs at the two resonant dips at 1242 nm and 1314 nm and a peak at 1284 nm are plotted as insets in Fig. 2(b). As for first transmission dip $\lambda_1=1242$ nm, nearly all the magnetic field is located in the upper cavity, and almost no electromagnetic field is detected at the end of the bus waveguide. For the second transmission dip, it indicates that a pump centered at $\lambda_2=1314$ nm can be trapped efficiently in the lower resonator, which leads to an extremely low transmission. It is known that there is a proportional relationship between the effective length L_{eff} of the resonant cavity and the wavelength λ_m of trapped resonant mode, which is clearly confirmed from the field image. Similar results can be also found in Ref. [18,30], which is better for realizing the relationship between resonant wavelength λ_m and effective cavity length L_{eff}.

For transmission dip $\lambda_3=1284$ nm, the electromagnetic fields of the upper and lower DURs are in opposite phase. Field distribution is detected at the end of the bus waveguide which is related to the transmission peak of 0.68. What can be understood is that the main reason for the occurrence of the transmission peak is related to the circumstance that the two U-resonators resonate out of phase with each other at the intermediate frequency λ_3.Then the incident light can propagate through the structure uninhibitedly due to the destructive interference between the electromagnetic fields in the two resonators which results in a transmission transparency window centered at 1284 nm with full width at half maximum(FWHM) 52 nm.

3.3. Influence of varied detuned wavelength in back coupled DURs

Since the detuned wavelength can result in a PIT-like phenomenon, we further investigate the varied detuning of resonant wavelengths on PIT-like feature in back coupled DURs. There are four groups of L_{i1} and L_{i2}, and i is equal to (1, 2, 3 and 4),where arm length L_{11}, L_{21}, L_{31}, L_{41} and L_{12}, L_{22}, L_{32}, L_{42} are 100 nm, 110 nm, 115 nm, 125 nm and 150 nm, 140 nm, 135 nm, 125 nm, respectively, which are related to the resonant frequencies. Considering the fact that $t_n-r_n=1$ and $\omega_n=2\pi c/\lambda_n$ ($n=1,2$), Eq. 3 can be rewritten as

$$T=\frac{1}{1+\frac{1}{4}\left(\frac{\Delta\lambda_1}{\lambda-\lambda_1}+\frac{\Delta\lambda_2}{\lambda-\lambda_2}\right)^2} \tag{4}$$

Here, $\Delta\lambda_1$ and $\Delta\lambda_2$ are the FWHM of both up and down U-resonators when they are singly located, respectively. Since $1/Q_o \ll 1/Q_e$, the relation $1/Q_t=1/Q_o+1/Q_e$ can be approximated to$1/Q_t=1/Q_e$. We discuss the transmission of the transparency peak in $(\lambda_1+\lambda_2)/2$ [29] when there is a wavelength detuning of $\delta=\lambda_2-\lambda_1$. Making $\lambda=(\lambda_1+\lambda_2)/2$, the formula in the bracket can be derived as $2(\Delta\lambda_2-\Delta\lambda_1)/(\lambda_2-\lambda_1)=2(\Delta\lambda_2-\Delta\lambda_1)/\delta$, here, FWHM difference $\Delta\lambda_2-\Delta\lambda_1$ is assumed to be constant due to the gradually increasing δ and low intrinsic loss of gold. Then it can be concluded from Eq. (4) that the total transmission efficiency T possesses a proportional relation to the wavelength detuning δ from the theoretical analysis.

So we can estimate that when wavelength detuning δ increases gradually, leading to a broader transparency window, the value of T may increase accordingly; on the contrary, the value of T decreases as δ becomes smaller. These deductions are confirmed by the following simulation analysis.

As it is shown in Fig. 3(a), transmission spectra of fundamental mode for varied δ_i are plotted in a coordinate. What can be discovered from Fig. 3(a) is that as the detuning δ_i decreases, the short wavelength dip comes to a redshift while blueshift for the long wavelength dip, which results in a much narrower transparency window with higher QF (quality-factor). Different QF and transmission maxima for transparency window in varied detuned structures are illustrated in Fig. 3(b), while transmission spectra for $L_1=105$ nm, $L_2=145$ nm and $L_1=120$ nm, $L_2=130$ nm are not shown for clarity. That means the width of the transparency window is highly sensitive to the frequency spacing between the resonance $\delta_i=\lambda_{i2}-\lambda_{i1}$, which can be tuned by adjusting the effective length of the DURs, similar to that shown in Ref. [30]. On the other hand, due to the metal internal loss, the transmission peak decreases accordingly. Compared with the study of side-coupled complementary split-ring resonators in Ref. [23], the extinction ratio of the transmission spectra of this research is about 0.89, which is much higher than 0.44–0.78 of that in the reference.

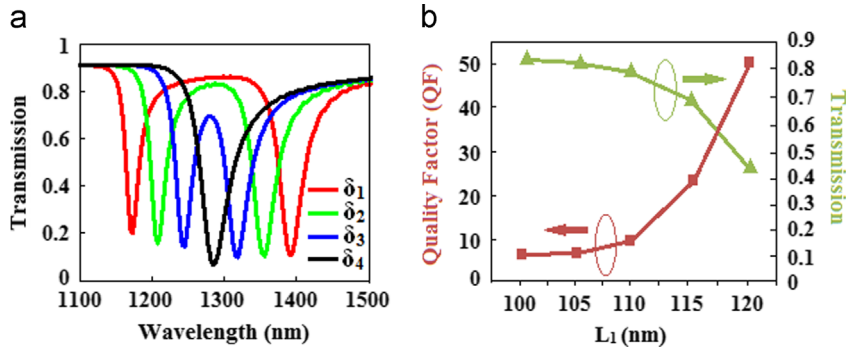

Fig. 3. (Color online) (a) Transmission spectra of fundamental mode with various wavelength detuning: $\delta_1=213$ nm, $\delta_2=145$ nm, $\delta_3=72$ nm and $\delta_4=0$ nm in the coupled MDM system with $L=280$ nm, $w=50$ nm and $d=20$ nm. The arm length (L_1 and L_2) are set as: 100 nm and 150 nm (red), 110 nm and 140 nm (green),115 nm and 135 nm (blue), 125 nm and 125 nm (black). (b)The quality factor change of transparency window for different degree of detuning (red curve) and its corresponding maximum transmission (green curve).

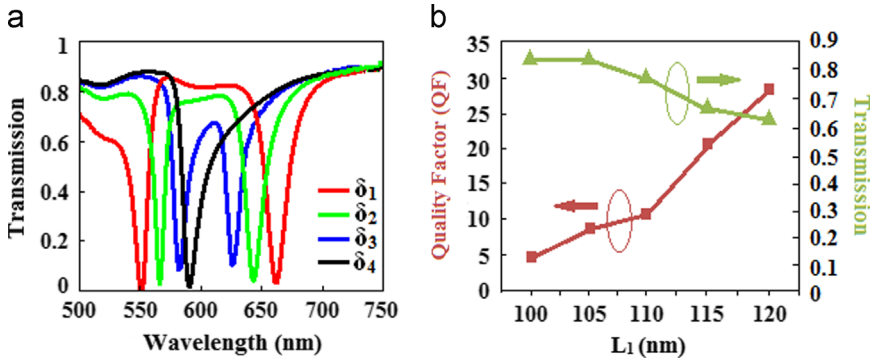

Fig. 4. (Color online) (a) Transmission spectra of second order mode with various wavelength detuning: $\delta_1=113$ nm, $\delta_2=78$ nm, $\delta_3=44$ nm, and $\delta_4=0$ nm in the coupled MDM system with the same structural parameters and graphic markers set in Fig. 3, respectively. (b)The quality factor change of transparency window for different degree of detuning (red curve) and its corresponding maximum transmission (green curve).

For fully understanding the PIT-like feature in our structure, the second order mode is considered in Fig. 4(a). The general changes in the spectra are similar to the fundamental mode except that sensitivity of the long wavelength is much sharper than that of the short wavelength. The relation of QF and transmission maxima for transparency window is also plotted in Fig. 4(b), while the variation trend is less apparent when comparing with the first order mode after $L_1=115$ nm.

The generated transparency mechanism for our research here can be attributed to the destructive interference between the electromagnetic fields in both up and down resonators while bright–dark mode mechanism leads to destructive interference of two different excitation pathways in the reference mentioned above. That means variation in mechanisms for PIT-like effect may possess different optical properties. The transparency window is much more sensitive to the proposed parameters, such as the arm length L_1 and L_2 of the DURs and with a bit higher QF. What can be inferred from the schematic is that there is a trade-off between the QF and transmission maxima for transparency window, which means high transmission usually comes with a relatively lower QF, and how to get high value for both of them still attracts researches. These effective characters are significant for potential applications in designing plasmonic and sensitive devices. When $L_1=L_2=125$ nm, there is only one transmission dip, which is related to the circumstance that the two DURs resonate in phase with each other at the intermediate frequency λ_3. Then the incident pulse cannot propagate through the structure uninhibitedly due to the constructive interference between the electromagnetic fields in the two DURs, so the incident beam is trapped which results in a transmission dip centered at 1284 nm.

Finally, an important issue to be considered is related to the expected phenomenon of slow-light propagation, for example, the analysis of high group indexes that can be achieved in our structure, which is just similar to the slow light effect in the atomic system [31,32].

In order to investigate the slow light effect in our system, we introduce an approximate treatment, the group index for the detuned back coupled U-resonators structures can be evaluated as follows [33]: $n_g=\lambda^2/(4t\Delta\lambda)$, where λ represents the central resonant wavelength of the transparency window, t is the length of the MDM waveguide and $\Delta\lambda$ is the full width at half maximum(FWHM) of the transparency window. For varied detuned wavelength U-resonators, t equals to 1000 nm as a constant and the calculated n_g for fundamental order mode is presented in Fig. 5. For different values of L_1, n_g is varied, the highest n_g value is about 16, which means a relatively slow group velocity of incident photons can be slower down in a velocity of $c/16=0.0625c$, where c stands for the velocity of light in vacuum. Another information that can be achieved from Fig. 5 is that, the group index increases as the detuning decreases. At the beginning, the enhancement of n_g is not obvious, but when L_1 comes to 110 nm, n_g increases rapidly. This may guarantee an even higher group index by further decreasing δ. The group velocity is almost two orders lower than c, which means the pronounced slow light effect can be applied in slow-light systems and devices, especially optical buffers.

4. Conclusion

In conclusion, we have investigated plasmonic analog of plasmon induced transparency numerically and theoretically in integrated plasmonic devices using detuned U-resonators indirectly back coupled with the MDM waveguide due to the near field of the evanescent wave. The theoretical result agrees well with the numerical one, which

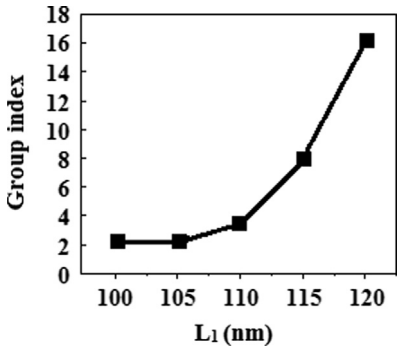

Fig. 5. Approximately calculated group index n_g for varied detuned structure.

provides a simple modified theoretical method for understanding PIT-like effect in coupled system. Both the fundamental and second order modes are considered for better realization. The sensitivity of wavelength and the trade-off trend between *Q*-factor and transmission maxima to the structure detuning for both modes varies accordingly. Those observations make the optical properties in our system tunable, which may be beneficial for future application. A group index of 16 can be achieved at near-infrared wavelength which guarantees a group velocity nearly two orders lower than *c*. It can be applied in nano-filters, slow-light systems and devices such as optical buffers.

Acknowledgments

Fundamental Research Funds for the Central Universities of Central South University No. 72150050429' is added. Then the final complete acknowledgment turn out to be: 'This work was supported by the Fundamental Research Funds for the Central Universities of Central South University No. 72150050429, the Research Fund for the Doctoral Program of Higher Education of China under Grant No. 20100162110068, the National Natural Science Foundations of China Grant No. 61275174.' We sincerely hope that it can be modified in the final publication in Solid State Communications.

References

[1] W. Cai, U.K. Chettiar, A.V. Kildishev, V.M. Shalaev, Nature Photonics 1 (2007) 224.
[2] B. Kanté, A. de Lustrac, J.M. Lourtioz, S.N. Burokur, Optics Express 16 (2008) 9191.
[3] B. Kanté, S.N. Burokur, A. Sellier, A. de Lustrac, J.M. Lourtioz, Physical Review B 79 (2009) 075121.
[4] N. Papasimakis, V.A. Fedotov, N.I. Zheludev, Physical Review Letters 101 (2008) 253903.
[5] C.L. Garrido-Alzar, M.A.G. Martinez, P. Nussenzveig, American Journal of Physics **70** (2002) 37.
[6] S.E. Harris, Physics Today 50 (1997) 36.
[7] B Tang, L Dai, C Jiang, Optics Express 19 (2011) 628.
[8] X.R. Jin, Y.H. Lu, J.W. Park, H.Y. Zheng, F. Gao, Y.P. Lee, J.Y. Rhee, K.W. Kim, H. Cheong, W.H. Jang, Journal of Applied Physics 111 (2012) 073101.
[9] W.L. Barnes, A. Dereux, T.W. Ebbesen, Nature (London) 424 (2003) 824.
[10] S.I. Bozhevolnyi, V. Volkov, E. Devaux, J. Laluet, T. Ebbesen, Nature (London) 440 (2006) 508.
[11] Q.Q. Gan, Y. Gao, Q. Wang, L. Zhu, F. Bartoli, Physical Review B 81 (2010) 085443.
[12] H. Lu, X. Liu, D. Mao, Physical Review A 85 (2012) 053803.
[13] Y.F. Xiao, X.B. Zou, W. Jiang, Y.L. Chen, G.C. Guo, Physical Review A 75 (2007) 063833.
[14] P. Tassin, L. Zhang, T. Koschny, E.N. Economou, C.M. Soukoulis, Optics Express 17 (2009) 5595.
[15] R.D. Kekatpure, E.S. Barnard, W.S. Cai, M.L. Brongersma, Physical Review Letters 104 (2010) 243902.
[16] P. Tassin, L. Zhang, T. Koschny, E.N. Economou, C.M. Soukoulis, Physical Review Letters 102 (2009) 053901.
[17] R. Singh, C. Rockstuhl, F. Lederer, W. Zhang, Physical Review B 79 (2009) 085111.
[18] Y. Huang, C.J. Min, G. Veronis, Applied Physics Letters 99 (2011) 143117.
[19] M. Fleischhauer, A. Imamoglu, J.P. Marangos, Reviews of Modern Physics 77 (2005) 633.
[20] Q. Xu, S. Sandhu, M.L. Povinelli, J. Shakya, S. Fan, M. Lipson, Physical Review Letters 96 (2006) 123901.
[21] Q. Li, T. Wang, Y.K. Su, M. Yan, M. Qiu, Optics Express 18 (2010) 8367.
[22] G Wang, H Lu, X Liu, Optics Express 20 (2012) 20902.
[23] Y. Guo, L. Yan, W. Pan, B. Luo, K. Wen, Z. Guo, X. Luo, Optics Express 20 (2012) 24348.
[24] M.A. Ordal, L.L. Long, R.J. Bell, S.E. Bell, R.R. Bell, R.W. Alexander, C.A. Ward, Applied Optics 22 (1983) 1099.
[25] A. Taflove, S.C. Hagness, Computational Electrodynamics: The Finite-Difference- Time-Domain Method, 2nd ed., Artech House, Boston, 2000.
[26] S.I. Bozhevolnyi, Optics Express 14 (2006) 9467.
[27] Q. Zhang, X. Huang, X. Lin, J. Tao, X. Jin, Optics Express 17 (2009) 7549.
[28] Z.H Han, Photonics and Nanostructures – Fundamentals and Applications 8 (2010) 172.
[29] Z.H Han, S.I Bozhevolnyi, Optics Express 19 (2011) 3251.
[30] Y. Gong, X. Liu, L. Wang, Y. Zhang, Optics Communications 284 (2011) 795.
[31] L.V. Hau, S.E. Harris, Z. Dutton, C.H. Behroozi, Nature 397 (1999) 594.
[32] Y. Rostovtsev, O. Kocharovskaya, G.R. Welch, M.O. Scully, Optics & Photonics News 13 (2002) 44.
[33] J. Zhang, W. Bai, L. Cai, Y. Xu, G. Song, Q. Gan, Applied Physics Letters 99 (2011) 181120.